

Attenuation of Bleomycin-Induced Pulmonary Fibrosis by a Catalytic Antioxidant Metalloporphyrin

Tim D. Oury, Kailas Thakker, Margaret Menache, Ling-Yi Chang, James D. Crapo, and Brian J. Day

Department of Pathology, University of Pittsburgh, Pittsburgh, Pennsylvania; Analytical Solutions, Raleigh, North Carolina; Department of Pediatrics, University of New Mexico, Albuquerque, New Mexico, Department of Medicine, National Jewish Medical & Research Center, and Departments of Medicine, Cell Biology, and Pharmaceutical Sciences, University of Colorado Health Sciences Center, Denver, Colorado

Oxidative stress plays an important role in the development of fibrotic responses in the lung. However, it is not clear whether inhibiting oxidative stress with antioxidants can attenuate fibrotic processes in the lung. The objective of these studies was to test whether the catalytic antioxidant porphyrin manganese (III) tetrakis (4-benzoic acid) porphyrin (MnTBAP) could protect mice against bleomycin-induced lung fibrosis. A 10 mg/kg intraperitoneal dose of MnTBAP was established as safe and had a serum and lung half-life of 9.5 h in mice. Based on this data, four groups of mice were given one dose of bleomycin (3.2 U/kg, intratracheal) or saline and MnTBAP (5 mg/kg, intraperitoneal) or saline twice daily for 14 d. Lung fibrosis was assessed by measuring (1) lung hydroxyproline content as an index of collagen accumulation, (2) airway dysfunction by whole body plethysmography, and (3) histopathology. Bleomycin produced a 20% loss in body weight that was only 10% in the bleomycin/MnTBAP group. Bleomycin produced a twofold increase in hydroxyproline content that was decreased 23% by MnTBAP. Bleomycin produced a twofold increase in airway dysfunction that was also attenuated 30% by MnTBAP. Histopathologic analysis of the lungs of mice treated with bleomycin demonstrated a severe fibrotic response that was attenuated 28% by MnTBAP. Future studies on the oxidant mechanisms that MnTBAP is affecting in this bleomycin model of lung fibrosis may shed light on potential new therapeutic approaches for treating interstitial lung diseases.

Interstitial pulmonary fibrosis is characterized by an altered cellular composition of the alveolar region with excessive deposition of collagen. The etiology of this disease is unknown; however, lung inflammation is a major underlying component of a wide variety of pulmonary fibroproliferative disorders. Reactive oxygen species (ROS), such as superoxide, hydrogen peroxide, peroxynitrite, and hydroxyl radical, are major mediators of lung inflammatory processes (1). Many xenobiotics that stimulate the overproduction of ROS, such as oxygen and paraquat (2), butylated hydroxytoluene (3), and bleomycin (4), are capable of producing lung fibrosis. Yet, the direct linkage of ROS formation and pulmonary fibrosis has not been firmly established.

Bleomycin is a commonly used chemotherapeutic agent that can cause dose-dependent pulmonary fibrosis (5). Bleo-

mycin has been extensively used in animal models of interstitial lung disease and it produces an acute lung injury response followed by lung fibrosis (6). The lung is selectively affected because this tissue lacks an enzyme that hydrolyzes the β -aminoalanine moiety of bleomycin, which prevents its metabolite from binding metals such as iron (7). Bleomycin can bind metal ions and DNA at the same time at two different sites, and this complex can generate ROS such as superoxide and hydroxyl radicals (8). The ability of bleomycin to bind both iron and DNA is thought to selectively target ROS toward DNA over other biomolecules such as proteins and lipids. Bleomycin produces DNA strand breakages that are lung specific and can be stimulated with exposure to oxygen in mice (9). The DNA strand breakage by bleomycin can be inhibited *in vitro* by the addition of a variety of antioxidants, such as superoxide dismutase (10), glutathione (11), and dimethylurea (12).

The role of ROS in many disease states has led to the development of metalloporphyrin catalytic antioxidants. Manganese (III) meso-tetrakis (4-benzoic acid) porphyrin (MnTBAP) is a stable metalloporphyrin that can catalyze the dismutation of superoxide (13) and hydrogen peroxide (14), scavenge peroxynitrite (15), and inhibit lipid peroxidation (16). MnTBAP has been shown to protect DNA from ROS-mediated strand breaks (15) and, more recently, protect mitochondrial DNA from ROS-mediated damage (17). Given the broad range of antioxidant activities of metalloporphyrins, it was of interest to examine their efficacy in an animal model of pulmonary fibrosis. The goal of these studies was to determine if the catalytic antioxidant MnTBAP could protect mice from bleomycin-induced lung fibrosis. MnTBAP was found to attenuate all parameters used to assess bleomycin-induced lung fibrosis by 20 to 30%.

Materials and Methods

Preparation of MnTBAP

A 1.5-M excess of manganese chloride (Fisher, Fair Lawn, NJ) was incubated with tetrakis-(4-benzoic acid) porphyrin (H_2TBAP) (Aldrich, Milwaukee, WI) that was dissolved in water and the pH titrated to 7.0 with 0.1 N sodium hydroxide. The reaction mixture was stirred and heated to 80°C. The pH of the reaction was monitored every hour and readjusted to 7.0 with 0.1 N sodium hydroxide. Metal ligation was followed spectrophotometrically (UV-2101 PC; Shimadzu, Columbia, MD). Over time, the Soret band for the H_2TBAP ($\lambda = 415$ nm) disappeared with the emergence of the Soret band for MnTBAP ($\lambda = 468$ nm), which has an extinction coefficient of $\epsilon = 9.3 \times 10^4 M^{-1} cm^{-1}$ (18). Excess metal was removed by batch adsorption with chelex-100 resin (BioRad, Hercules, CA). The product was passed through a 0.22- μm filter (Millipore, Bedford, MA) and stored in the dark at 4°C until

(Received in original form May 5, 2000 and in revised form April 4, 2001)

Address correspondence to: Brian J. Day, Ph.D., K706A Goodman Bldg., National Jewish Medical and Research Center, 1400 Jackson St., Denver, CO 80206. E-mail: DAYB@NJ.C.ORG

Abbreviations: high performance liquid chromatography, HPLC; manganese (III) meso-tetrakis (4-benzoic acid) porphyrin, MnTBAP; phosphate-buffered saline, PBS; enhanced pause, P_{ENH} ; reactive oxygen species, ROS; standard error of the mean, SEM.

Am. J. Respir. Cell Mol. Biol. Vol. 25, pp. 164–169, 2001
Internet address: www.atsjournals.org

used. The purity of the MnTBAP was found to be greater than 90% by high performance liquid chromatography (HPLC) analysis. MnTBAP was tested for endotoxin content using a kinetic QCL inhibition/enhancement test (BioWhittaker, Walkersville, MD) and was found to contain less than 5 ng endotoxin/mg MnTBAP.

Animals and Treatments

Balb/c male mice that were 6 to 8 wk of age were used in these studies (Taconic, Germantown, NY). Mice were acclimated to 22°C in an environmentally controlled room (12-h light cycles) at least 6 d before treatment. Toxicity studies were employed using a moving average method previously described by Weil (19). Four groups of four mice were given MnTBAP (50, 88, 153, and 268 mg/kg, intraperitoneally) and observed over a 48-h time period. Mice were given one bolus dose of MnTBAP (10 mg/kg, intraperitoneally) dissolved in phosphate-buffered saline (PBS) and blood and lung tissue levels of MnTBAP were determined at several different time points for pharmacokinetic analysis. Separate sets of mice were used for the lung fibrosis study. Mice were randomized into two groups of 10 mice that received intratracheal bleomycin (3.5 U/kg; ICN, Aurora, OH) or an equivalent volume of saline (50 μ l). Half the animals in these groups also received MnTBAP (5 mg/kg, intraperitoneally) or an equivalent volume of PBS (1 ml/kg, intraperitoneally) twice daily for 14 d. Animal use was reviewed and approved by an Animal Use Committee, which follows recommended guidelines reported in the *Guide for the Care and Use of Laboratory Animals*.

Analysis of MnTBAP in Serum and Lung Homogenates

Mice were anesthetized with pentobarbital (60 mg/kg, intraperitoneally), and blood was obtained by a cardiac puncture. Blood samples were placed in 1.5-ml tubes and left at room temperature to clot for 30 min. Serum was removed after spinning the blood samples at $1,000 \times g$ for 10 min. Serum samples were stored at -20°C until used. Lungs were perfused with PBS through the pulmonary artery to clear blood from the vasculature. The lungs were removed and homogenized in 10 mM Tris-HCl buffer containing 1.15% potassium chloride at pH 7.5 with a polytron (Turrax-25; Janke & Kunkel, Staufen, Germany). Lung homogenates were stored at -20°C until used. MnTBAP was extracted from serum (50 μ l) and lung homogenates (100 μ l) with 800 μ l of methanol, vortexed for 2 min, and centrifuged at $7,000 \times g$. The top layer was removed, and the extraction process was repeated twice. The pooled fractions were evaporated to dryness and redissolved in 100 μ l of water. This substance was then transferred to HPLC vials for analysis. Standards were prepared in control lung or serum samples and extracted as described previously. MnTBAP was quantitated using an HPLC (Ranin, Emeryville, CA) equipped with an ultraviolet-1 detector set at $\lambda = 468$ nm and a flow rate of 1 ml/min. The stationary phase consisted of a YMC ODS C-18 column (1.4 \times 100 mm) and a mobile phase consisting of 60% solution A and 40% solution B (solution A: water + 0.1% trifluoroacetate; solution B: acetonitrile/water [90:10] + 0.1% trifluoroacetate). MnTBAP extracted from lung homogenates and serum eluted at 5.9 min. Recovery of MnTBAP from samples using the extraction method described previously ranged from 85 to 91%. The linear regression analysis of the standard curves were $r^2 > 0.99$.

Pharmacokinetics

A standard, two-compartment model was used to calculate serum and tissue half-life (20). The data were fitted to the following equation: $C_d = Ae^{-at} + Be^{-bt}$, where a and b are rate constant for the distribution phase and elimination phase, respectively. The constants A and B are intercepts on the y -axis for each exponential segment of the curve. The constant B was used as an estimate of the peak serum and lung MnTBAP levels, respectively. The cal-

culated values were computer generated from Prizm 3.0 (GraphPad, San Diego, CA).

Noninvasive Measurement of Airway Dysfunction in Mice

The baseline enhanced pause (P_{ENH}) in unrestrained, conscious mice was assessed by whole body barometric plethysmography (Buxco Electronics, Troy, NY). The techniques used were similar to those described by Zhu and coworkers (21). Mice were placed in whole body plethysmographs with fast differential transducers interfaced to a computer. Measurements were made of respiratory rates, tidal volumes, and P_{ENH} . Airway dysfunction was expressed as $P_{ENH} = [(T_e/0.3T_r) - 1] \times [2P_{ef}/3P_{if}]$, where T_e = expiratory time (seconds), T_r = relaxation time (seconds), P_{ef} = peak expiratory flow (milliliters/second), and P_{if} = peak inspiratory flow (milliliters/second). Animals were allowed to equilibrate in the chambers for 15 min, and then P_{ENH} was calculated over a 5-min period using a running average.

Hydroxyproline Measurement

The left lung was dried at 80°C until a constant weight was obtained. The dried lung was hydrolyzed under vacuum in a glass vial in 1 ml of 12 N HCl at 120°C overnight. The samples were lyophilized and assayed for hydroxyproline content using chloramine-T as previously described (22).

Histopathology

The lungs were fixed in 4% paraformaldehyde for 24 h and then processed for paraffin embedding. Sections of lung were stained with routine hematoxylin and eosin or with a Masson trichrome stain to assess the degree of fibrosis. The extent of lung injury and fibrosis was graded by a pathologist (T.D.O.), blinded as to the treatment group, on a scale of 0 for normal lung to 8 for severe distortion of structure and large tissue areas as previously reported by Ashcroft and colleagues (23). The major criteria examined included interstitial thickening of alveolar or bronchiolar walls, collagen deposition, and inflammatory cell infiltration.

Statistical Analyses

Data were analyzed using a two-way analysis of variance (ANOVA). Significant differences between groups were assessed using a Newman-Keuls multiple comparison test. Data were analyzed using the computer program Prizm (GraphPad). Scoring data were analyzed (SASV6.12) using a two-way ANOVA. Statistically significant effects were tested by Bonferroni corrected t test. Statistical significance was set at $P < 0.05$.

Results

Toxicity and Pharmacokinetic Assessment of MnTBAP in Mice

To test the efficacy of the catalytic antioxidant MnTBAP (Figure 1) in a model of pulmonary fibrosis, we first needed to establish a dosing regimen that would result in MnTBAP lung levels without drug toxicity. MnTBAP toxicity was assessed using a moving average method that consisted of four geometric dose groups (50, 88, 153, and 268 mg/kg, intraperitoneally) of four mice each over 48 h. There were no deaths associated with the 50 mg/kg group and one death in the 88 mg/kg group. The two highest doses were lethal to the mice. MnTBAP had a calculated LD_{50} of 100 mg/kg with a 95% confidence interval of 98 to 104 mg/kg. We then choose a 10-mg/kg intraperitoneal injection of MnTBAP to conduct pharmacokinetic studies based on the toxicity data. Serum and lung tissue levels of MnTBAP were

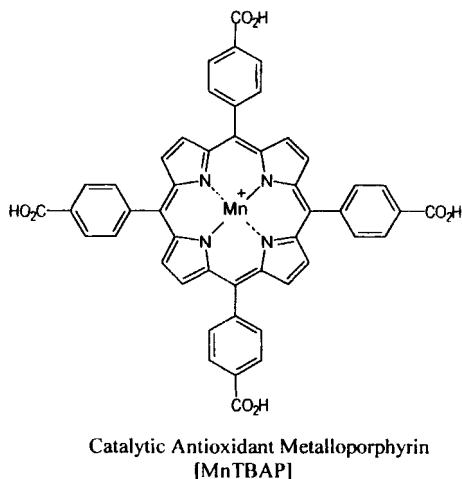


Figure 1. Chemical structure of a catalytic antioxidant, MnTBAP, is shown.

determined at 0.3, 0.5, 1, 2, 4, 6, and 24 h after drug treatment. The data were fitted to a two-compartment pharmacokinetic model, and the distribution and elimination half-lives were calculated from the data fitted curves (Figure 2). MnTBAP rapidly equilibrated into the lung from the bolus intraperitoneal injection with a distribution half-life of 14 min (Table 1). The estimated peak serum and lung tissue concentration of MnTBAP was 42 mg/liter and 80 $\mu\text{g/g}$ protein, respectively. The elimination half-lives of MnTBAP from the serum and lung were identical at 9.5 h. This information suggests that (1) MnTBAP does not accumulate in the lung and (2) using a twice-a-day dosing regimen based on its half-life of 9.5 h.

Attenuation of Bleomycin-Induced Lung Fibrosis by MnTBAP

Mice were randomized into four groups using a two-by-two contingency table where two groups received either saline

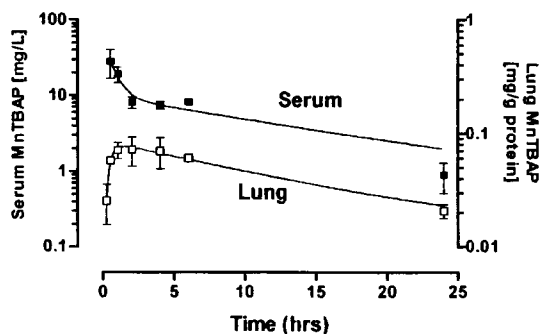


Figure 2. The pharmacokinetic profile of MnTBAP in mice given a single 10 mg/kg, intraperitoneal dose. MnTBAP levels in serum (solid squares) and lung tissue (open squares) were measured at 0.3, 0.5, 1, 2, 4, 6, and 24 h after drug treatment. Results are expressed as the mean of three mice \pm SEM. Data were calculated from curve-fitted data assuming a two-compartment pharmacokinetic model. MnTBAP rapidly equilibrated into the blood stream and the lungs of mice.

TABLE 1
Pharmacokinetic profile of MnTBAP
(10 mg/kg, intraperitoneal) in mice

	Peak Level (C_o)	Distribution Half-life ($T_{1/2}, \text{min}$)	Elimination Half-Life ($T_{1/2}, \text{h}$)
Serum	42 mg/liter	27	9.5
Lung	80 $\mu\text{g/g}$ protein	14	9.5

or bleomycin (3.5 U/kg body weight) by intratracheal instillation. Two groups also received either saline or MnTBAP (5 mg/kg body weight) by intraperitoneal injection twice daily for 14 d. The groups that received bleomycin lost significantly more weight than did vehicle control mice over 14 d with a maximum average loss of 20% of their initial body weight (Figure 3). MnTBAP treatment did not cause weight loss as compared with the saline control group. The group of mice that received both bleomycin and MnTBAP had less weight loss than did the bleomycin group from Days 5 to 14 with a maximum average loss of 10%.

Bleomycin given by intratracheal instillation produces a marked airway and alveolar fibrotic response (24). Mice were assessed for changes in airway function by measuring a marker, $PENH$, of airway dysfunction using noninvasive whole body barometric plethysmography. Intratracheal instillation of bleomycin treatment produced a threefold increase in the $PENH$ index of airway dysfunction after 14 d (Figure 4A). MnTBAP treatment alone did not affect the $PENH$ marker but caused a 30% decrease in airway dysfunction produced by bleomycin treatment. Lung fibrosis was also assessed by measuring hydroxyproline content in the lung as an index of collagen accumulation. Bleomycin treatment produced a twofold increase in hydroxyproline content of the lung after 14 d (Figure 4B). MnTBAP treatment had little effect on hydroxyproline content of the lung but produced a 23% decrease in hydroxyproline content caused by bleomycin treatment. Increases in both $PENH$ and hydroxyproline content correlated well with fibrotic changes seen by histopathologic assessment.

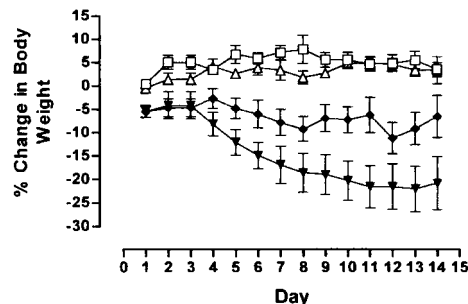


Figure 3. MnTBAP attenuates bleomycin-induced weight loss in mice. Control (PBS, 1 ml/kg, intraperitoneal, twice daily; open squares) and MnTBAP-treated (5 mg/kg, intraperitoneal, twice daily; open triangles) mice had similar weight changes throughout the study period. Bleomycin-treated (solid triangles) mice had significantly more weight loss than control mice, and this was attenuated in the bleomycin plus MnTBAP-treated (solid diamonds) mice after 5 d of treatment and continued to the end of the study. Results are expressed as the mean of five mice \pm SEM.

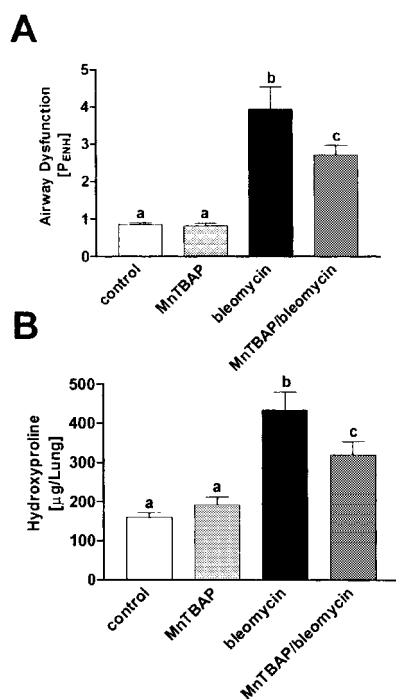


Figure 4. MnTBAP attenuates bleomycin-induced airway constriction and collagen accumulation. (A) Whole body barometric plethysmography was employed and P_{ENH} was used as a noninvasive index of airway dysfunction. Control (PBS, 1 ml/kg, intraperitoneal, twice daily; *open bar*) and MnTBAP-treated (5 mg/kg, intraperitoneal, twice daily; *hatched bar*) mice had similar P_{ENH} values after 14 d of treatment. Bleomycin-treated (*solid bar*) mice had significantly elevated P_{ENH} values compared with control mice, and this was attenuated in the bleomycin plus MnTBAP-treated (*cross-hatched bar*) mice. (B) Lung fibrosis was biochemically assessed using hydroxyproline as an index of collagen accumulation. Control (*open bar*) and MnTBAP-treated (*hatched bar*) mice had similar hydroxyproline values after 14 d of treatment. Bleomycin-treated (*solid bar*) mice had significantly elevated hydroxyproline values compared with control mice, and this was attenuated in the bleomycin plus MnTBAP-treated (*cross-hatched bar*) mice. Results are expressed as the mean of five mice \pm SEM. Bars with different letters are significantly different from one another, $P < 0.05$.

One lung from each mouse was fixed with 4% paraformaldehyde by intratracheal instillation and embedded in paraffin for histopathologic assessment. Tissue sections were stained with hematoxylin and eosin or with Masson trichrome stain to assess the degree of lung injury/fibrosis. Bleomycin treatment produced an inflammatory response characterized by substantial thickening and loss of normal alveolar structure, type 2 cell hyperplasia, and an intense acute inflammatory response in alveolar and interstitial spaces (Figure 5A) as compared with control lungs (Figure 5A). Lung sections from bleomycin-treated animals stained for collagen with a trichrome stain showed marked increased collagen accumulation, predominately in the thickened alveolar regions and to a lesser extent around small bronchioles (Figure 5G), compared with control lungs (Figure 5E). MnTBAP treatment alone had no effect on lung histology (Figures 5B and 5F) but attenuated the marked interstitial

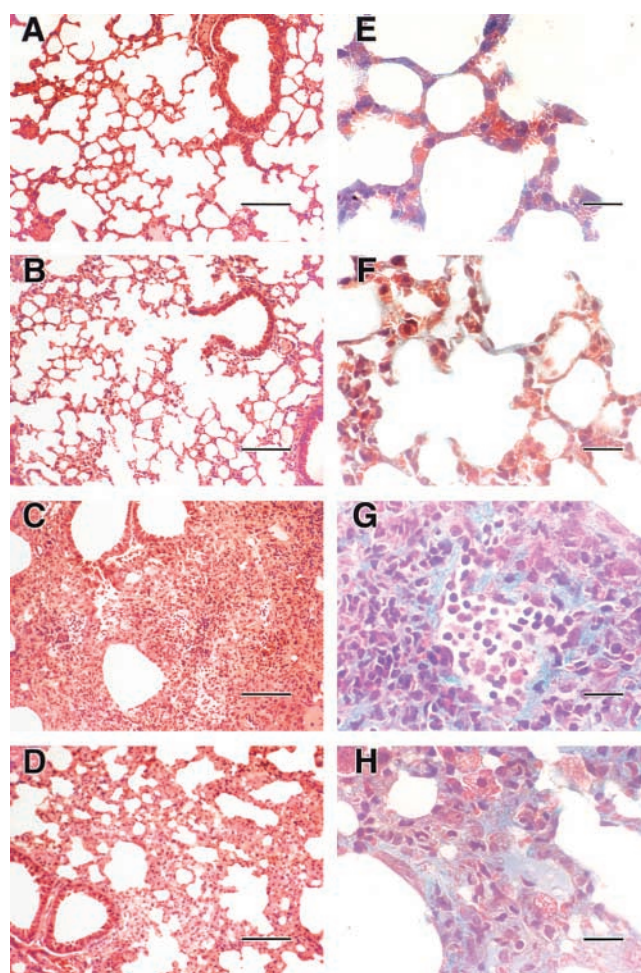


Figure 5. MnTBAP attenuates bleomycin-induced pulmonary injury. Mice were treated with PBS (1 ml/kg, intraperitoneal, twice daily for 14 d), MnTBAP (5 mg/kg, intraperitoneal, twice daily for 14 d, bleomycin (3.5 U/kg, intratracheal, once), or bleomycin plus MnTBAP and killed after 14 d. Lungs were inflation fixed in 10% neutral-buffered formalin. Five-micron-thick sections were stained with hematoxylin and eosin and examined microscopically. (A) Representative lung section from a PBS/PBS-treated mouse. (B) Representative lung section from a PBS/MnTBAP-treated mouse. (C) Representative lung section from a bleomycin/PBS-treated mouse. (D) Representative lung section from a bleomycin/MnTBAP-treated mouse. Bar = 100 μm . Five-micron-thick sections were stained with Masson trichrome and examined microscopically. (E) Representative lung section from a PBS/PBS-treated mouse. (F) Representative lung section from a PBS/MnTBAP-treated mouse. (G) Representative lung section from a bleomycin/PBS-treated mouse. (H) Representative lung section from a bleomycin/MnTBAP-treated mouse. Bar = 20 μm .

thickening and inflammatory responses produced by bleomycin (Figure 5D) and also decreased the collagen accumulation as assessed by trichrome staining (Figure 5H). Lung sections were semiquantitatively assessed for fibrotic response on a scale of 0 to 8, with a score of zero representing a normal lung and a score of eight representing a very severe fibrotic lung, as previously described by Ashcroft and associates (23). Lung sections were randomized and scored blind. Bleomycin treatment produced a two-

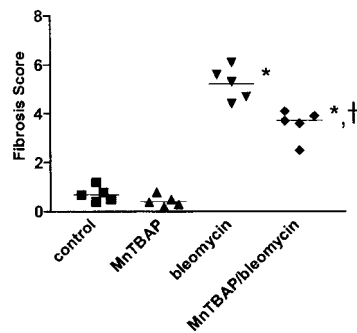


Figure 6. MnTBAP attenuates bleomycin-induced lung injury as determined by histopathologic analysis. Mice were treated with either bleomycin (3.5 U/kg, intratracheal) or PBS (50 μ l), and then given MnTBAP (5 mg/kg, intraperitoneal, twice daily) or PBS (1 ml/kg, intraperitoneal, twice daily) for 14 d. Lungs were inflated fixed in 10% neutral-buffered formalin.

Five-micron-thick sections were stained with hematoxylin and eosin or Masson Trichrome and examined microscopically. Slides were systematically scanned on a microscope using a $\times 10$ objective. Each successive field was individually assessed for severity of interstitial fibrosis and allotted a score between 0 and 8 using a predetermined scale of severity as described in the MATERIALS AND METHODS. Scores from the fields were averaged to obtain the pathologic score for each animal. Bars with asterisks are statistically different from the PBS/PBS group ($P < 0.05$). A dagger indicates a significant interaction between MnTBAP and bleomycin ($P < 0.05$). Solid squares, solid triangles, and solid diamonds indicate different treatment groups.

fold increase in the pathology score as compared with the control group (Figure 6). MnTBAP treatment had no effect on the pathology score but attenuated the bleomycin pathology score by 28%. The statistical analysis indicated a significant interaction between the bleomycin and MnTBAP treatments ($P = 0.01$). These results closely support the physiologic and biochemical indices where bleomycin produced about a twofold increase in the various indices and MnTBAP attenuated these increases by roughly 30%.

Discussion

This study provides a pharmacokinetic profile of the catalytic antioxidant MnTBAP, showing that it can be delivered to the lung from an intraperitoneal injection with a half-life of approximately 10 h, allowing for a twice-a-day dosing regimen. In addition, this information was applied to a bleomycin model of pulmonary lung injury/fibrosis, and MnTBAP was found to attenuate the bleomycin-induced injury response in mice. Specifically, MnTBAP (10 mg/kg/d) was found to attenuate bleomycin-induced weight loss, collagen accumulation, airway dysfunction, and injury by 20 to 50%.

Animal models do not completely mimic the interstitial lung disease in humans and usually require an acute lung injury response followed by a slower fibrosis phase that differs from the chronic and insidious features of this disease in humans. Inflammation is a major component in the pathogenesis of interstitial lung disease that is orchestrated in part by endogenous and migrating leukocytes. These leukocytes together with lung epithelial and endothelial cells create a feedback loop where stimuli from injury responses can activate alveolar and interstitial macrophages (25). Activated leukocytes can release reactive oxygen and nitrogen species (superoxide, hydrogen peroxide, hydroxyl radical, hypochlorous acid, nitric oxide, and peroxynitrite) and proteases that sustain the injury/repair processes that are thought to contribute to the fibrotic processes (26). The

scenario creates an approach to break the feedback loop by using catalytic antioxidants such as MnTBAP that can scavenge a broad spectrum of reactive oxygen and nitrogen species. Oxidants may alter the structure of target proteins to render them more susceptible to proteolytic attack and may inactivate antiproteases as well as activate latent proteinases that are crucial in collagen remodeling in the lung (27). MnTBAP has been successfully used to prevent injury responses in activated macrophages (15) and is an effective agent in preventing oxidant-induced injury responses both *in vitro* and *in vivo* (13, 28).

Bleomycin-induced fibrosis is the most commonly used animal model and appears as a significant drug-induced lung disease in the clinical setting (29). Genetic backgrounds of mice contribute to the degree and intensity of lung injury induced by bleomycin. In these studies, a more resistant strain of mice, Balb/c, was used to limit the mortality seen in the bleomycin model with the more commonly used sensitive strain, C57/B6. Common features of bleomycin-induced lung injury include marked hyperplasia and metaplasia of type II cells and a pleiomorphic inflammatory infiltrate in the interstitial and alveolar spaces (30). Alveolar inflammation is a major component of the initial inflammatory processes, and the thickened interstitium results from its repair. MnTBAP treatment attenuated these typical changes in the alveolar regions, but significant fibrotic areas still remained and collagen accumulation was only attenuated by 20%. These data suggest that the major effects of MnTBAP were on decreasing the initial injury responses triggered by bleomycin. Other groups have also reported similar effects of agents thought to diminish the initial injury response of bleomycin (31).

The presence and severity of fibrosis likely depends on the severity and protraction of the initial lung injury induced by bleomycin. Reactive oxygen and nitrogen species have been implicated in lung injury caused by combining bleomycin and hyperoxia results in a synergistic development of pulmonary injury characterized by diffuse alveolar damage and interstitial fibrosis (32). In addition, administration of manganese superoxide dismutase (MnSOD) inhibited bleomycin-induced fibrosis, further implicating a role of superoxide in mediating bleomycin-induced lung injury (31). MnTBAP has superoxide dismutase activity (33) and can substitute for MnSOD in knockout mice (34). Iron deficiency also blunts bleomycin-induced injury and lipid peroxidation, suggesting iron-catalyzed oxygen radicals may be responsible for the initial injury response. MnTBAP is a potent inhibitor of iron-mediated lipid peroxidation (16) and may be providing some protection through this mechanism as well. The ability of bleomycin to bind both iron and DNA is thought to selectively target ROS toward DNA over other biomolecules such as proteins and lipids. MnTBAP can protect DNA from hydrogen peroxide-mediated damage (17) as well as from oxidants generated from leukocyte activation (15). Work is currently under way looking at markers of oxidant injury in MnTBAP/bleomycin-treated lungs to better understand which mechanisms are important in its protective effects. Clearly, there is probably a host of nonoxidant mechanisms also at play in the fibrotic processes that limit the efficacy of a catalytic antioxidant in this model.

Disruption of mitochondrial function may be a novel aspect of fibroproliferative disorders. Niacin and nicotinamide have also been found to attenuate fibrosis induced by bleomycin (4). The mechanism of protection is not known but speculated to be due to an inhibitory effect on the initial lung injury response by maintaining nicotinamide adenine dinucleotide levels, and thus adenosine triphosphate levels, required for repair of damaged epithelial cells. These results are intriguing and may implicate a mitochondrial metabolic dysfunction as part of the fibrotic process. MnTBAP can protect mitochondrial targets against oxidative damage and may also be working indirectly to preserve mitochondrial function (17, 28). Mitochondrial dysfunction as a process of aging has been thought to be a critical element in many late onset diseases (35). Given the late onset of idiopathic pulmonary fibrosis and the ability of oxidants to produce fibrotic changes in the lung, there is a distinct possibility that this may be a disease associated with mitochondrial degeneration.

In summary, the catalytic antioxidant MnTBAP may prove a valuable tool in our understanding the role of oxidant mechanisms in pulmonary fibrosis. MnTBAP can be delivered to animals in a reasonable dosing regimen that can attenuate the accumulation of collagen, lung dysfunction, weight loss, and lung pathology associated with an animal model of pulmonary fibrosis. Future studies to identify which oxidant mechanisms MnTBAP is affecting in the bleomycin model may shed light on potential new therapeutic approaches for the fatal lung disease known as idiopathic pulmonary fibrosis.

Acknowledgments: The authors thank Dr. Dan Costa for his helpful discussions and comments, and Boyd Jacobson and Tanya Canafax for their excellent technical assistance. This study was supported in part by grants HL59602 (B.J.D.) and HL31992 (J.D.C.) from the National Institutes of Health, by grant DA-001-N from the American Lung Association (T.D.O.), by a CMRF grant from the University of Pittsburgh Medical Center (T.D.O.), and by a grant from Aeolus Pharmaceuticals, Inc. (B.J.D., J.D.C.).

References

- Kinnula, V. L., J. D. Crapo, and K. O. Raivio. 1995. Generation and disposal of reactive oxygen metabolites in the lung. *Lab. Invest.* 73:3-19.
- Selman, M., M. Montano, C. Ramos, R. Barrios, and R. Perez-Tamayo. 1989. Experimental pulmonary fibrosis induced by paraquat plus oxygen in rats: a morphologic and biochemical sequential study. *Exp. Mol. Pathol.* 50:147-166.
- Adamson, I. Y., D. H. Bowden, M. G. Cote, and H. Witschi. 1977. Lung injury induced by butylated hydroxytoluene: cytodynamic and biochemical studies in mice. *Lab. Invest.* 36:26-32.
- Wang, Q. J., S. N. Giri, D. M. Hyde, and C. Li. 1991. Amelioration of bleomycin-induced pulmonary fibrosis in hamsters by combined treatment with taurine and niacin. *Biochem. Pharmacol.* 42:1115-1122.
- Luna, M. A., C. W. Bedrossian, B. Lichtiger, and P. A. Salem. 1972. Interstitial pneumonitis associated with bleomycin therapy. *Am. J. Clin. Pathol.* 58:501-510.
- Szapiel, S. V., N. A. Elson, J. D. Fulmer, G. W. Hunninghake, and R. G. Crystal. 1979. Bleomycin-induced interstitial pulmonary disease in the nude, athymic mouse. *Am. Rev. Respir. Dis.* 120:893-899.
- Filderman, A. E., L. A. Genovese, and J. S. Lazo. 1988. Alterations in pulmonary protective enzymes following systemic bleomycin treatment in mice. *Biochem. Pharmacol.* 37:1111-1116.
- Gutteridge, J. M., and F. Xiao Change. 1981. Protection of iron catalysed the radical damage to DNA and lipids by copper (II) bleomycin. *Biochem. Biophys. Res. Commun.* 99:1354-1360.
- Sogal, R. N., A. A. Gottlieb, A. R. Boutros, R. R. Ganapathi, R. R. Tubbs, P. Satariano, P. R. Blakely, and G. J. Beck. 1987. Effect of oxygen on bleomycin-induced lung damage. *Cleve. Clin. J. Med.* 54:503-509.
- Galvan, L., C. H. Huang, A. W. Prestayko, J. T. Stout, J. E. Evans, and S. T. Crooke. 1981. Inhibition of bleomycin-induced DNA breakage by superoxide dismutase. *Cancer Res.* 41(12, Pt. 1):5103-5106.
- Poli, P., A. Buschini, A. Candi, and C. Rossi. 1999. Bleomycin genotoxicity alteration by glutathione and cytochrome P-450 cellular content in respiratory proficient and deficient strains of *Saccharomyces cerevisiae*. *Mutagenesis.* 14:233-238.
- Trush, M. A., E. G. Mimnaugh, E. Ginsburg, and T. E. Gram. 1982. Studies on the interaction of bleomycin A2 with rat lung microsomes: II. Involvement of adventitious iron and reactive oxygen in bleomycin-mediated DNA chain breakage. *J. Pharmacol. Exp. Ther.* 221:159-165.
- Day, B. J., S. Shawen, S. I. Liochev, and J. D. Crapo. 1995. A metalloporphyrin superoxide dismutase mimetic protects against paraquat-induced endothelial cell injury, *in vitro*. *J. Pharmacol. Exp. Ther.* 275:1227-1232.
- Day, B. J., I. Fridovich, and J. D. Crapo. 1997. Manganic porphyrins possess catalase activity and protect endothelial cells against hydrogen peroxide-mediated injury. *Arch. Biochem. Biophys.* 347:256-262.
- Szabo, C., B. J. Day, and A. L. Salzman. 1996. Evaluation of the relative contribution of nitric oxide and peroxynitrite to the suppression of mitochondrial respiration in immunostimulated macrophages using a manganese mesoporphyrin superoxide dismutase mimetic and peroxynitrite scavenger. *FEBS Lett.* 381:82-86.
- Day, B.J., I. Batinic-Haberle, and J. D. Crapo. 1999. Metalloporphyrins are potent inhibitors of lipid peroxidation. *Free Radic. Biol. Med.* 26:730-736.
- Milano, J., and B. J. Day. 2000. A catalytic antioxidant metalloporphyrin blocks hydrogen peroxide-induced mitochondrial DNA damage. *Nucleic Acids Res.* 28:968-973.
- Harriman, A., and G. Porter. 1979. Photochemistry of manganese porphyrins. *J. Chem. Soc. Faraday Trans.* 275:1532-1542.
- Weil, C.S. 1952. Tables for convenient calculation of median-effective dose (LD₅₀ or ED₅₀) and instructions in their use. *Biometrics* 8:249-263.
- Shargel, L., and A. B. Yu. 1980. Applied Biopharmaceutics and Pharmacokinetics. New York: Appleton-Century-Crofts, New York.
- Zhu, Z., R. J. Homer, Z. Wang, Q. Chen, G. P. Geba, J. Wang, Y. Zhang, and J. A. Elias. 1999. Pulmonary expression of interleukin-13 causes inflammation, mucus hypersecretion, subepithelial fibrosis, physiologic abnormalities, and eotaxin production. *J. Clin. Invest.* 103:779-788.
- Woessner, J. F. 1961. The determination of hydroxyproline in tissue and protein samples containing small proportions of this amino acid. *Arch. Biochem. Biophys.* 93:440-447.
- Ashcroft, T., J. M. Simpson, and V. Timbrell. 1988. Simple method of estimating severity of pulmonary fibrosis on a numerical scale. *J. Clin. Pathol.* 41:467-470.
- Evans, J. N., J. Kelley, R. B. Low, and K. B. Adler. 1982. Increased contractility of isolated lung parenchyma in an animal model of pulmonary fibrosis induced by bleomycin. *Am. Rev. Respir. Dis.* 125:89-94.
- Hunninghake, G. W., J. I. Gallin, and A. S. Fauci. 1978. Immunologic reactivity of the lung: the *in vivo* and *in vitro* generation of a neutrophil chemotactic factor by alveolar macrophages. *Am. Rev. Respir. Dis.* 117:15-23.
- Henson, P. M., and R. B. Johnston, Jr. 1987. Tissue injury in inflammation: oxidants, proteinases, and cationic proteins. *J. Clin. Invest.* 79:669-674.
- Shabani, F., J. McNeil, and L. Tippett. 1998. The oxidative inactivation of tissue inhibitor of metalloproteinase-1 (TIMP-1) by hypochlorous acid (HOCl) is suppressed by anti-rheumatic drugs. *Free Radic. Res.* 28:115-123.
- Patel, M., B. J. Day, J. D. Crapo, I. Fridovich, and J. O. McNamara. 1996. Requirement for superoxide in excitotoxic cell death. *Neuron.* 16:345-355.
- Jules-Elysee, K., and D. A. White. 1990. Bleomycin-induced pulmonary toxicity. *Clin. Chest Med.* 11:1-20.
- Fleischman, R. W., J. R. Baker, G. R. Thompson, U. H. Schaeppli, V. R. Ilievski, D. A. Cooney, and R. D. Davis. 1971. Bleomycin-induced interstitial pneumonia in dogs. *Thorax* 26:675-682.
- Parizada, B., M. M. Werber, and A. Nimrod. 1991. Protective effects of human recombinant MnSOD in adjuvant arthritis and bleomycin-induced lung fibrosis. *Free Radic. Res. Commun.* 15:297-301.
- Tryka, A. F., J. J. Godleski, W. A. Skornik, and J. D. Brain. 1983. Progressive pulmonary fibrosis in hamsters. *Exp. Lung Res.* 5:155-171.
- Weinraub, D., P. Levy, and M. Faraggi. 1986. Chemical properties of water-soluble porphyrins: 5. Reactions of some manganese (III) porphyrins with the superoxide and other reducing radicals. *Int. J. Radiat. Biol. Relat. Stud. Phys. Chem. Med.* 50:649-658.
- Melov, S., J. A. Schneider, B. J. Day, D. Hinerfeld, P. Coskun, S. S. Mirra, J. D. Crapo, and D. C. Wallace. 1998. A novel neurological phenotype in mice lacking mitochondrial manganese superoxide dismutase [see comments]. *Nat. Genet.* 18:159-163.
- Beal, M. F. 1995. Aging, energy, and oxidative stress in neurodegenerative diseases. *Ann. Neurol.* 38:357-366.